Basic Study on Received Power Control of In-Flight Inductive Power Transfer for Drones by Active Rectifier Switching and Altitude Regulation

1st Yusuke Satoh
Graduate School of Frontier Sciences
The University of Tokyo
Kashiwa, Chiba, Japan
sato.yusuke22@ae.k.u-tokyo.ac.jp

2nd Kota Fujimoto
Graduate School of Frontier Sciences
The University of Tokyo
Kashiwa, Chiba, Japan
fujimoto.kota21@ae.k.u-tokyo.ac.jp

3rd Ryo Matsumoto
Graduate School of Frontier Sciences
The University of Tokyo
Kashiwa, Chiba, Japan
matsumoto.ryo19@ae.k.u-tokyo.ac.jp

4th Nguyen Binh Minh
Graduate School of Frontier Sciences
The University of Tokyo
Kashiwa, Chiba, Japan
nguyen.binhminh@edu.k.u-tokyo.ac.jp

5th Sakahisa Nagai
Graduate School of Frontier Sciences
The University of Tokyo
Kashiwa, Chiba, Japan
nagai-saka@edu.k.u-tokyo.ac.jp

6th Hiroshi Fujimoto
Graduate School of Frontier Sciences
The University of Tokyo
Kashiwa, Chiba, Japan
fujimoto@k.u-tokyo.ac.jp

***Abstract*—The short flight time is one of the problems hindering the development of industrial applications of drones. As a solution to this problem, in-flight wireless power transfer (WPT) has been attracting attention, especially in security and R&D operations. One of the challenges of in-flight WPT for drones is the received power control due to fluctuations of mutual inductance and the motor's required power. Usually, in WPT applications, the active rectifier is used to control the received power. When the received power is excessive, the active rectifier keep switching to control the power received. However, that switching deteriorates the system efficiency. Conversely, if there is not enough power, a normal WPT system cannot control power only by receiving side. In the in-flight WPT system, on the other hand, the freedom of altitude and the ability to actively adjust mutual inductance can be applied to power control. In this paper, we propose a unique received power control for in-flight drones that combines power control by the rectifier and altitude control. The performance improvements have been experimentally demonstrated on the bench system. As a result, the AC-DC efficiency on the secondary side improved by $4.10\,\%$ because of a reduction in the number of switching times of the rectifier. When received power was insufficient, the current increased by $1\,\mathrm{A}$ and exceeded the lower limit of the control target.**

***Index Terms*—wireless power transfer, drone, power control, altitude control, semi-bridgeless active rectifier**

I. Introduction

In recent years, drones have been used in various fields. On the other hand, drones face a significant problem in terms of short flight time. Accordingly, wireless power transfer (WPT) for in-flight drones has been proposed to solve this problem [1]. WPT has attracted attention because of its convenience of not requiring wires, and research is underway to improve the safety, stability, and efficiency [2]–[4]. In particular, as shown in Fig. 1, this paper assumes the system that directly feeds power to a drone flying in a straight line at a constant speed over primary coils arranged in series, which is helpful for missions such as security and R&D operations, where the drone is mainly operated along a fixed route or location. It also enables continuous flight and reduces the number of drones. In addition, since the above situation involves flying at low altitudes, inductive power transfer (IPT), which enables high-efficiency and high-power transmission, is considered suitable as a power supply method for drones [5].

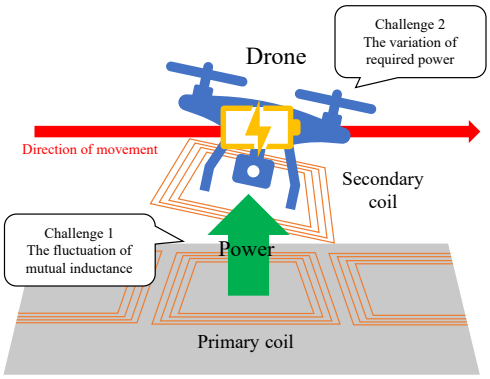

Fig. 1. WPT for in-flight drones using the magnetic resonance coupling.

However, the following two challenges must be overcome to realize desired power transfer on the in-flight WPT system. The first challenge is that the mutual inductance of the coils might vary depending on relative positions between the primary and secondary coil, possibly causing unstable power charging. The second challenge is that the desired power by drones is time-varying, depending on the operation mode. In addition, the desired power also relies on the total mass, which could be varied due to the load of the drones.

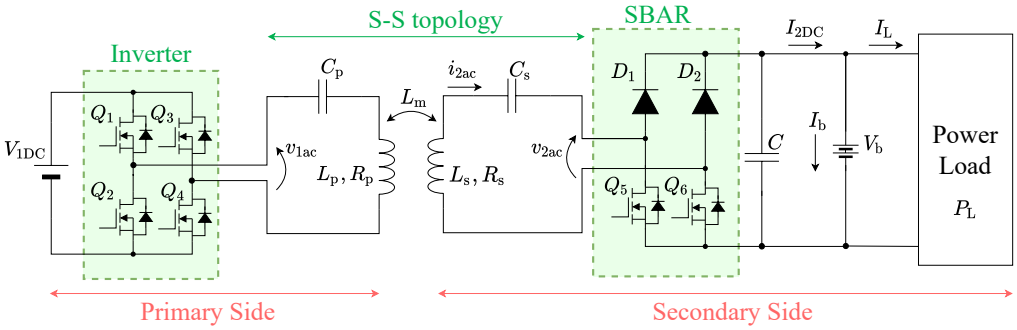

Fig. 2. Overall view of the circuit.

There are two methods for receiving power control: one is based on the estimation of the mutual inductance [6] [7], and the other is based on control the DC voltage on the primary side [8]. The former requires the values of circuit parameters such as inductance and resistance to be known, and cannot cope with parameter fluctuations due to aging or manufacturing errors. The latter requires communication between the transmitter and receiver, which increases the weight of drones and causes communication delays.

There is also research on using an active rectifier to control the power received [9]. By controlling the switching of the rectifier's MOSFETs, the current overshoot can be suppressed and the output voltage can be controlled at a constant voltage. However, the high-speed switching of the MOSFETs causes high switching losses.

With respect to the aforementioned challenges, this paper proposes a new power control method with an active rectifier without communication delay for improving the efficiency on in-flight WPT systems. The proposal can be summarized as follows.

1) By adjusting the mutual inductance with altitude control of the drone, the required power can be provided regardless of circuit parameter deviations.
2) By the received power control based on the altitude adjustment, the semi-bridgeless active rectifier (SBAR) can be operated with minimum switching of the MOSFETs, thus reducing the switching loss.

II. Circuit Configuration

This section describes the circuit configuration of the magnetic resonance coupling WPT used in this paper. The overall view of the WPT circuit is shown in Fig. 2. In this paper, the S-S topology is adopted. L, R, and C represent the self-inductance, the internal resistance, and the capacitance, respectively. The subscripts p and s represent the primary side and the secondary side, respectively. Q and D represent the MOSFET and the diode, respectively. V_1DC and V_b represent the input voltage and the battery voltage, respectively. P_L represents the power load that simulates the drone motor. L_m denotes the mutual inductance. Also, the SBAR is used as the rectifier on the secondary side [10]. Compared to full-bridge active rectifiers, the SBAR can be operated with a more simple configuration and its lighter trait is suitable for WPT in drones, where weight reduction is desirable.

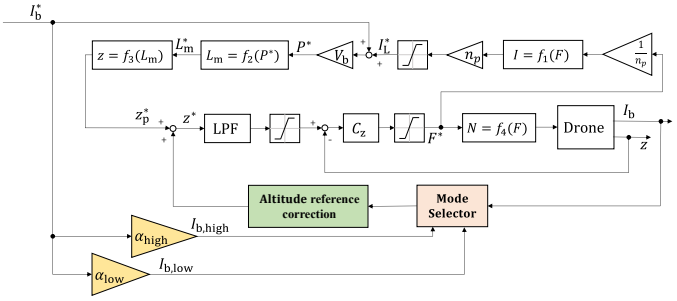

Fig. 3. Block diagram of flight altitude and battery current control.

III. Battery Current Control Using Flight Altitude and SBAR Switching

This section describes the control method proposed in this paper. The block diagram representing the overall control algorithm is shown in Fig. 3. The battery current is controlled using PI control with a SBAR. The details are described in Subsections Ⅲ-A and Ⅲ-C. The upper threshold $I_\mathrm{b,high}$ and lower threshold $I_\mathrm{b,low}$ are decided based on the average reference current I_b^* as $I_\mathrm{b,high} = \alpha_\mathrm{high} I_\mathrm{b}^*$, $I_\mathrm{b,low} = \alpha_\mathrm{low} I_\mathrm{b}^*$. In this paper, α_high and α_low are set to $\pm 10\%$ to account for variations in motor current. The reference value for PI control is set to $I_\mathrm{b,high}$. f_1 represents the relationship between the required thrust for the desired flight F and the drone's motor current I_L. For simplicity, we assume that the drone does not tilt and that the power requirements of all motors are the same. f_2 shows the relationship between the drone's desired power P^* and mutual inductance L_m, expressed by the theoretical equation described in Section Ⅲ-B. f_3 is experimentally determined relation between L_m and the flight altitude z. f_4 shows the relationship between F and motor speed N. C_z represents the PID altitude controller, and LPF represents the low-pass filter. n_p is the number of propellers.

A. Battery Current Control by SBAR

The SBAR can switch between rectification mode (Fig. 4(a)) and short mode (Fig. 4(b)) by the gate signal of the MOSFETs

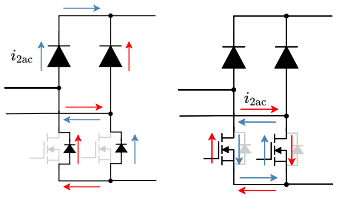

(a) Rectification mode (b) Short mode

Fig. 4. Operation mode of SBAR.

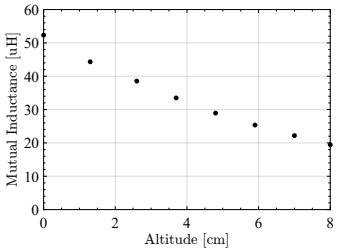

Fig. 5. Relationship between altitude and mutual inductance.

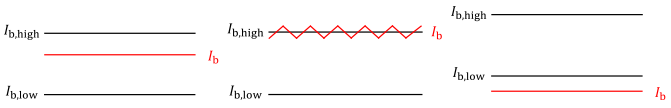

(a) Always rectification mode (b) Switching mode (c) Current shortage mode

Fig. 6. Current waveforms in each operation mode.

in the lower arm [11] [12]. In this paper, the battery current is controlled by creating the gate signal using the PI controller and switching the SBAR's operation mode. The detailed control algorithm is explained in Section Ⅲ-C. The SBAR can reduce the receiving current by the ratio of the rectification-mode period and short-mode period. When the number of the mode switching increases, the system efficiency deteriorates. By combining the altitude control, the number of the mode switching can be reduced.

B. Determination of Reference for Flight Altitude Control Based on Circuit Model

In the flight altitude control, first, based on the WPT circuit model, the theoretical flight altitude to transfer the required power in only rectification mode is calculated, and the drone is controlled to that altitude. Next, to minimize modeling errors, the flight altitude is adjusted so that the required power can be achieved using only the rectification mode.

By solving the circuit equations derived from Fig. 2, the load impedance Z_{ac} can be expressed as

$$Z_{\mathrm{ac}} = \frac{v_{2\mathrm{ac}}}{i_{2\mathrm{ac}}} = \frac{8}{\pi^2}\frac{V_{\mathrm{b}}^2}{I_{\mathrm{b}}V_{\mathrm{b}} + P_{\mathrm{L}}}. \tag{1}$$

The received power P_{s} can be expressed as

$$P_{\mathrm{s}} = \frac{\omega^2 L_{\mathrm{m}}^2 Z_{\mathrm{ac}}}{(\omega^2 L_{\mathrm{m}}^2 + Z_{\mathrm{ac}}R_{\mathrm{p}} + R_{\mathrm{p}}R_{\mathrm{s}})^2} v_{1\mathrm{ac}}^2. \tag{2}$$

ω is the operating angular frequency of the primary inverter. As described in (2), the received power is changed by Z_{ac} and L_{m}. The SBAR can control Z_{ac} by the switching. L_{m} can be changed by the altitude control.

The reference of flight altitude controller is the value at which the drone can theoretically guarantee the required power P^* which is sum of the load power P_{L} and battery charging power P_{b} $(= V_{\mathrm{b}} \times I_{\mathrm{b}})$. Solving (2) for mutual inductance gives

$$L_{\mathrm{m}} = f_2(P^*) = \sqrt{\frac{-a + \sqrt{a^2 - 4\omega^4 b}}{2\omega^4}} \tag{3}$$

where

$$a = 2\omega^2(Z_{\mathrm{ac}}R_{\mathrm{p}} + R_{\mathrm{p}}R_{\mathrm{s}}) - \frac{\omega^2 Z_{\mathrm{ac}} v_{\mathrm{ac1}}^2}{P^*},$$
$$b = (Z_{\mathrm{ac}}R_{\mathrm{p}} + R_{\mathrm{p}}R_{\mathrm{s}})^2.$$

At first, the optimal mutual inductance to achieve the desired output power is calculated from (3). Secondly, the flight altitude is obtained from the pre-measured relationship between the altitude and mutual inductance as shown in Fig. 5.

C. Altitude Reference Correction to Maintain Always Rectification Mode

When the altitude is controlled to the reference described in Section Ⅲ-B, the battery current I_{b} may deviate from the theoretical value because of the modeling errors, such as aging, manufacturing errors, misalignment of the power receiving coil, and other factors. The three patterns of after initial altitude control are shown in Fig. 6. z_{ideal} is the altitude reference obtained from the desired power P^* using the functions f_2 and f_3 under conditions without parameter or modeling errors.

When adjusted reference of the altitude $z_{\mathrm{p}}^* = z_{\mathrm{ideal}}$, the battery current is shown in Fig. 6(a). This state is called "always rectification mode". When $z_{\mathrm{p}}^* > z_{\mathrm{ideal}}$, the battery current is shown in Fig. 6(b). This state is called "switching mode". In this mode, the SBAR is switched between rectification and short modes to regulate the output power. As a result, the switching loss of the MOSFETs increases compared to the "always rectification mode". Since this paper assumes drones as the application, heat generated by the rectifier due to the switching loss is undesirable, which makes it necessary to load heavy cooling devices on drones [13]. When $z_{\mathrm{p}}^* < z_{\mathrm{ideal}}$, the battery current is shown in Fig. 6(c). This state is called "power shortage mode". In power shortage mode, the battery charging speed is slower than ideal, which is not desired in the charging system.

In the proposed method, the flight altitude reference is corrected when the system is in switching or current shortage mode. The altitude is controlled so that the system finally operate in always rectification mode. By feeding the battery current to the "Mode Selector" block shown in Fig. 3, it is determined whether PI control is being performed or not. If

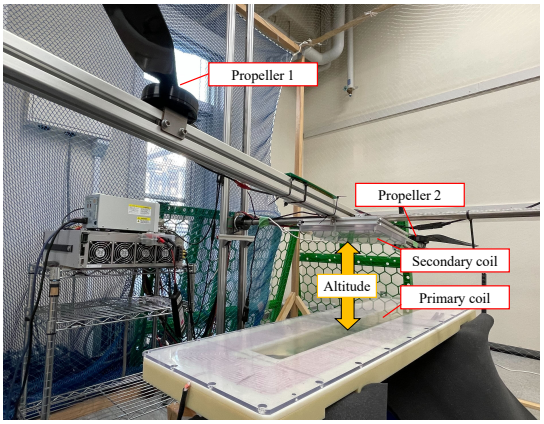

Fig. 7. Experimental bench simulating drone.

TABLE I
EXPERIMENT PARAMETERS.

Parameter	Value
$V_{1\mathrm{DC}}$	180 V
f	84.5 kHz
L_p	244.57 µH
R_p	303.65 mΩ
C_p	14.86 nF
L_s	86.25 µH
R_s	565.56 mΩ
C_s	40.56 nF
C	3900 µF
V_b	55 V
$I_\mathrm{b,high}$	11 A
$I_\mathrm{b,low}$	9 A
T_s	0.005 s
Δz_o	3.0×10^{-5} m

the battery current is oscillated between $I_\mathrm{b,low}$ and $I_\mathrm{b,high}$, the Mode Selector judge the condition as switching mode. If the battery current is under $I_\mathrm{b,low}$, the Mode Selector judge the condition as current shortage mode.

Then, in the case of switching mode, a step size of Δz_o is subtracted from the altitude reference z_p^* every control period of T_s. In current shortage mode, the altitude reference z_p^* is gradually increased by a step size of Δz_o. Finally, the altitude correction is completed when the mode becomes always rectification mode.

IV. EXPERIMENTAL RESULTS

Four experiments were conducted to show the usefulness of the proposed method. This experiment was conducted using a bench with two propellers as the drive system to simulate the drone as shown in Fig. 7. The circuit parameters of the WPT system are shown in Table I. In this experiment, battery voltage V_b was fixed without considering the change of the battery state of charge. Furthermore, the forward motion of the secondary coil was not performed in this study for simplicity and the experiment was limited to the vertical motion. The lateral displacement between the primary and secondary coil, as well as the yaw and roll movement of the drone, is not taken into account. The relationship between the altitude and mutual inductance between two coils in this experimental system is shown in Fig. 5.

A. Experiment 1 : Switching mode (w/o altitude control)

In Experiment 1, as shown in Fig. 8(a), the reference altitude value was not corrected and fixed at 7 cm. Since the instant value of I_b exceeds $I_\mathrm{b,high}$ at this time, the SBAR is in switching mode, which can be seen in Fig. 8(b)(c). I_b appears to be below $I_\mathrm{b,low}$, which may be due to the discontinuous state of the SBAR. In this study, it is acceptable because it is important to show a high switching frequency, but we plan to resolve this issue in future studies. In this experiment, the drone was hovering at a constant altitude, so the motor current shown in Fig. 8(d) remained approximately constant. The AC-DC efficiency, which is the rectifier conversion efficiency, was 86.17 %. It is assumed that the loss increased due to the constant high speed switching in the SBAR.

B. Experiment 2 : Current shortage mode (w/o altitude control)

In Experiment 2, as shown in Fig. 9(a), the reference altitude value was not corrected and the value was fixed at 3 cm. In this case, I_b was below $I_\mathrm{b,low}$, resulting in current shortage mode, which can be seen in Fig. 9(b). Therefore, the desired amount of power could not be transmitted, and in this condition, the battery charging time would be longer. The received power was 722.1 W. The drone was hovering at a constant altitude in this experiment the same as in Experiment 1, so the motor current shown in Fig. 9(c) was kept approximately constant.

C. Experiment 3 : Switching mode to Always rectification mode

In Experiment 3, as shown in Fig. 10(a), the initial value of the altitude reference was set to 7 cm and the reference correction described in Section Ⅲ-C was implemented. As can be seen from Fig. 10(b), I_b was initially in switching mode, so the altitude reference value decreased as it moved in the direction of reducing the received power. The motor current is smaller than in Experiments 1 and 2, as shown in Fig. 10(c), because of the decrease in the altitude reference value from the beginning. When the motor enters always rectification mode, the current increases in order to maintain a constant altitude. As a result, the SBAR is operated in always rectification mode where the battery current stays between $I_\mathrm{b,high}$ and $I_\mathrm{b,low}$ without switching the SBAR. The AC-DC efficiency was then raised from 86.98 % to 91.08 % in switching mode, resulting in an improvement of 4.10 %.

D. Experiment 4 : Current shortage mode to Always rectification mode

In Experiment 4, as shown in Fig. 11(a), the initial value of the altitude reference was set to 3 cm and reference correction was performed. As can be seen from Fig. 11(b), I_b was initially below $I_\mathrm{b,low}$, resulting in current shortage mode. Therefore, the altitude reference value was increased

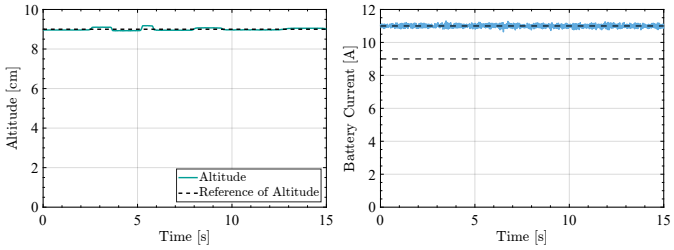

(a) Measured and reference value of altitude (b) Battery current waveform

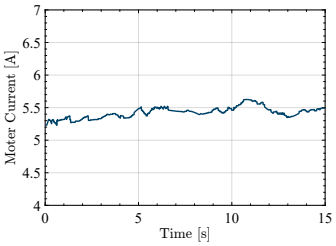

(c) Motor current waveform

Fig. 8. The result of Experiment 1 : switching mode (w/o correction).

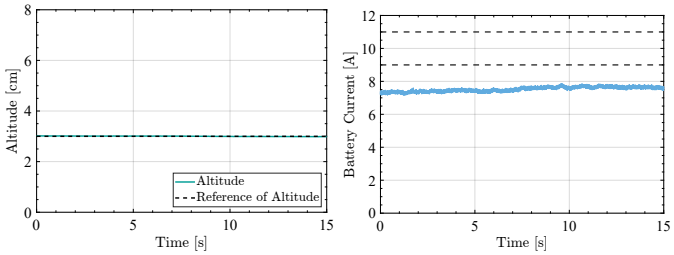

(a) Measured and reference value of altitude (b) Battery current waveform

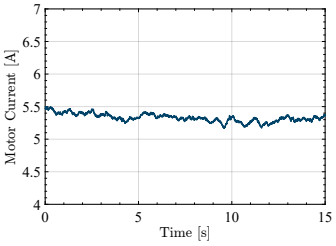

(c) Motor current waveform

Fig. 9. The result of Experiment 2 : current shortage mode (w/o correction).

to move in the direction of increasing the received power. As a result, I_{b} increased and settled between $I_{\mathrm{b,high}}$ and $I_{\mathrm{b,low}}$, resulting in always rectification mode. Regarding the motor current, it increases to a value greater than that in Experiments 1 and 2, as shown in Fig. 11(c), because the altitude reference value is increasing at first. When the motor enters the constant commutation mode, the current decreases in order to maintain a constant altitude. The received power then increased from $719.8\,\mathrm{W}$ in current shortage mode to $829.7\,\mathrm{W}$, which represents an increase of $109.9\,\mathrm{W}$.

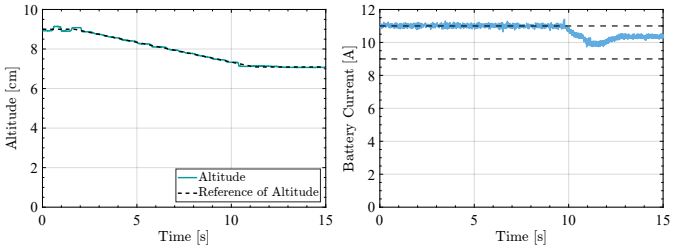

(a) Measured and reference value of altitude (b) Battery current waveform

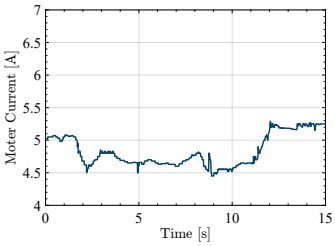

(c) Motor current waveform

Fig. 10. The result of Experiment 3 : switching to always rectification mode.

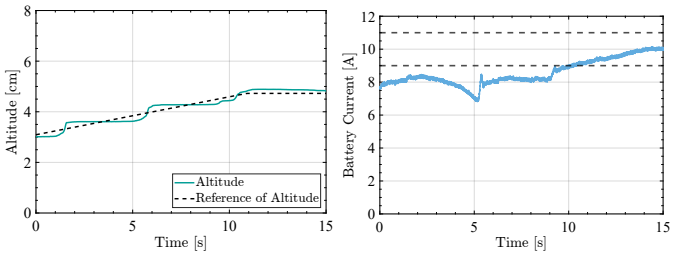

(a) Measured and reference value of altitude (b) Battery current waveform

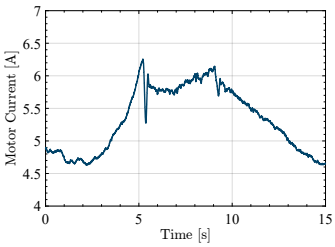

(c) Motor current waveform

Fig. 11. The result of Experiment 4 : current shortage to always rectification mode.

E. Transfer efficiency and received power in each experiment

The efficiency of each conversion stage and the received power for each experiment are shown in Table II. In Experiment 1, in which the SBAR was always operated at switching mode, the power was obtained satisfactorily at $831.9\,\mathrm{W}$, while the AC-DC efficiency was limited to a relatively low value of $86.17\,\%$. On the other hand, in Experiment 3, reference correction was performed and the transition from switching mode to always rectification mode improved the AC-DC efficiency by $4.10\,\%$ while realizing the desired power transfer. This is because the reduction of the switching losses in the SBAR, and the reduced losses will encourage smaller rectifier

TABLE II
TRANSFER EFFICIENCY AND RECEIVED POWER IN EACH EXPERIMENT.

Experiment	DC-AC	AC-AC	AC-DC	DC-DC	Received Power
1	98.88 %	84.76 %	86.17 %	72.22 %	831.9 W
2	92.00 %	85.73 %	90.28 %	77.40 %	722.1 W
3	98.12 % → 97.70 %	82.86 % → 84.56 %	86.98 % → 91.08 %	70.71 % → 75.25 %	847.1 W → 842.6 W
4	92.78 % → 97.78 %	85.22 % → 84.12 %	90.07 % → 90.07 %	71.26 % → 74.08 %	719.8 W → 829.7 W

cooling devices on the drone, leading to a reduction in overall drone weight.

In Experiment 2, the system always operated in current shortage mode, resulting in an AC-DC efficiency of 90.28 %, while the received power was insufficient at 722.1 W. On the other hand, in Experiment 4, the transition from current shortage mode to always rectification mode due to the reference correction increased the received power from 719.8 W to 829.7 W, which represents an increase of 109.9 W. This is expected to reduce battery charging time and result in a more efficient drone operation rate.

V. CONCLUSION

This paper proposes a method to control the receiving power and improve the system efficiency by the control of the flight altitude and the SBAR switching, assuming WPT for an in-flight drone. Experimental results show that the proposed method improves the AC-DC efficiency of the secondary side compared to the always switching control operation on SBAR. This reduces the heat generated by the rectifier, enabling the cooling system to be downsized and the drone to be lighter. It also moves the drone in the direction of eliminating power shortages. In the future study, the proposed method will be extended to take into account the variation in mutual inductance due to the forward movement of the drone. Both the altitude and the pitch angle are managed based on the integrated robust control system for in-forward-flight WPT system.

REFERENCES

[1] K. Fujimoto, T. Hamada and H. Fujimoto, "Proposal on Model Based Current Overshoot Suppression of Receiver Side Coil in Drone Wireless Power Transfer System," in *Proc. 2022 Wireless Power Week*, pp. 235-239, 2022.

[2] S. Y. R. Hui, Y. Yang and C. Zhang, "Wireless Power Transfer: A Paradigm Shift for the Next Generation," *IEEE Journal of Emerging and Selected Topics in Power Electronics*, vol. 11, no. 3, pp. 2412-2427, 2023.

[3] Z. Zhang, H. Pang, A. Georgiadis and C. Cecati, "Wireless Power Transfer—An Overview," *IEEE Transactions on Industrial Electronics*, vol. 66, no. 2, pp. 1044-1058, 2019.

[4] K. Chen, J. Pan, Y. Yang and K. W. E. Cheng, "Stability Improvement and Overshoot Damping of SS-Compensated EV Wireless Charging Systems With User-End Buck Converters," *IEEE Transactions on Vehicular Technology*, vol. 71, no. 8, pp. 8354-8366, 2022.

[5] G. Lovison, T. Imura, H. Fujimoto, Y. Hori, "Secondary-side-only Phase-shifting Voltage Stabilization Control with a Single Converter for WPT Systems with Constant Power Load," *IEEJ Journal of Industry Applications*, vol. 8, no. 1, pp. 66-74, 2019.

[6] Y. Gu, J. Wang, Z. Liang and Z. Zhang, "Mutual-Inductance-Dynamic-Predicted Constant Current Control of LCC-P Compensation Network for Drone Wireless In-Flight Charging," *IEEE Transactions on Industrial Electronics*, vol. 69, no. 12, pp. 12710-12719, 2022.

[7] J. Zeng, S. Chen, Y. Yang and S. Y. R. Hui, "A Primary-Side Method for Ultrafast Determination of Mutual Coupling Coefficient in Milliseconds for Wireless Power Transfer Systems," *IEEE Transactions on Power Electronics*, vol. 37, no. 12, pp. 15706-15716, 2022.

[8] H. Zhang, Y. Chen, C. H. Jo, S. J. Park and D. H. Kim, "DC-Link and Switched Capacitor Control for Varying Coupling Conditions in Inductive Power Transfer System for Unmanned Aerial Vehicles," *IEEE Transactions on Power Electronics*, vol. 36, no. 5, pp. 5108-5120, 2021.

[9] S. Zou, O. C. Onar, V. Galigekere, J. Pries, G. J. Su and A. Khaligh, "Secondary Active Rectifier Control Scheme for a Wireless Power Transfer System with Double-Sided LCC Compensation Topology," in *Proc. IECON 2018*, pp. 2145-2150, 2018.

[10] K. Colak, E. Asa, M. Bojarski, D. Czarkowski and O. C. Onar, "A Novel Phase-Shift Control of Semibridgeless Active Rectifier for Wireless Power Transfer," *IEEE Transactions on Power Electronics*, vol. 30, no. 11, pp. 6288-6297, 2015.

[11] D. Gunji, T. Imura and H. Fujimoto, "Stability analysis of constant power load and load voltage control method for Wireless In-Wheel Motor," in *Proc. 9th International Conference on Power Electronics and ECCE Asia*, pp. 1944-1949, 2015.

[12] S. Nagai, T. Fujita, H. Fujimoto, S. Tsuge and T. Hashimoto, "Efficiency Evaluation of Receiving Current Control Using Pulse Density Modulation for Dynamic Wireless Power Transfer," in *Proc. 2021 IEEE PELS Workshop on Emerging Technologies: Wireless Power Transfer*, pp. 1-5, 2021.

[13] J. Itoh, K. Mizoguchi, L. H. Nam and K. Kusaka : "Design Method of Cooling Structure Considering Load Fluctuation of High-power Wireless Power Transfer System," *Proc. 4th International Future Energy Electronics Conference*, pp. 1-6, 2019.